Calibration and experiments of discrete element flexible model parameters for kiwifruit stalk

Zhi He,[1,2,3] Xinting Ding,[1,2] Wei Hao,[1,3] Kai Li,[1,3] Weixin Gong,[1] Zixu Li,[1] Yongjie Cui[1,3]

[1]College of Mechanical and Electronic Engineering, Northwest A&F University, Yangling, Shaanxi; [2]Key Laboratory of Agricultural Internet of Things, Ministry of Agriculture and Rural Affairs, Yangling, Shaanxi; [3]Shaanxi Key Laboratory of Agricultural Information Perception and Intelligent Service, Yangling, Shaanxi, China

Abstract

A method combining experimental and simulation optimization was used to calibrate parameters to enhance the accuracy of discrete element model parameters during kiwifruit stem separation. First, physical experiments were conducted to determine the intrinsic and contact parameters of kiwifruit stalk. Second, the mechanical parameters of the kiwifruit stalks were determined using three-point bending and shear tests. On this basis, simulation tests were conducted on kiwifruit stalks by combining the Hertz-Mindlin model with a bonding model, and the optimal combination of bonding parameters was confirmed using the bending strength and maximum shear force. Finally, a discrete element model of the kiwifruit was built with the determined bonding parameters and simulated, and the reliability of the model was verified through mechanical tests. The results showed that the density was 867.5 kg/m^3, Poisson's ratio was 0.26, the modulus of elasticity was 3.25×10^8 Pa, the recovery coefficient between the fruit stalks and steel parts was 0.365, and the average values of the static and dynamic friction coefficients between the kiwifruit stalks and steel parts were 0.268 and 0.152, respectively. The kiwifruit stem bonding parameters were normal stiffness per unit area k_n=7.201×10^{11} N/m^3, shear stiffness per unit area k_t=2.379×10^{11} N/m3, critical normal stress σ_{max}=5.937×10^8 Pa, critical shear stress t_{max} = 2.354×10^9 Pa, and bonded disc radius R_j=0.164 mm. Compared with the results of the mechanical tests, the relative errors of the bending strength and maximum shear of the discrete element model were 2.13% and 2.84%, respectively. The results showed that the discrete element model improves the simulation of the bending and shearing processes of kiwifruit stalks and is capable of characterizing the physical properties of kiwifruit stalks. The results of this study provide a theoretical foundation for the optimal design of end effectors.

Correspondence: Yongjie Cui, College of Mechanical and Electronic Engineering, Northwest A&F University, Yangling, China. Tel. +86.29.87092391.
E-mail: agriculturalrobot@nwafu.edu.cn

Key words: kiwifruit stalks; discrete element; bonding model; parameter calibration.

Contributions: all the authors made a substantive intellectual contribution, performed part of the experiments. All the authors read and approved the final version of the manuscript and agreed to be accountable for all aspects of the work.

Conflict of interest: the authors declare that they have no known competing financial interests or personal relationships that could have appeared to influence the work reported in this paper.

Acknowledgments: this research has received support from the National Natural Science Foundation of China (31971805). The authors are also gratefully to the reviewers for their helpful comments and recommendations, which make the presentation better.

Received: 8 November 2023.
Accepted: 28 January 2024.

Journal of Agricultural Engineering 2024; LV:1640
doi:10.4081/jae.2024.1640

Introduction

Kiwifruit is favored by consumers and is widely grown for its richness of vitamin C (Suo *et al*., 2020). China has the largest kiwifruit cultivation area and production in the world, reaching 193,000 ha with an annual production of over 2.2 million tons in 2020 (He *et al*., 2022). However, the Chinese kiwifruit industry is still labor-intensive compared to developed countries, especially in terms of time-consuming and labor-intensive picking processes and postharvest treatment (Yuan *et al*., 2020). The application of agricultural machinery equipment for kiwifruit Post-harvesting and picking has contributed to alleviating the risk of seasonal labor shortages and reducing labor costs (Williams *et al*., 2019&2020), where harvesting kiwifruit with stalks is more beneficial for storage and transportation (Mu *et al*., 2018). The kiwifruit stalk, a vine-type stem, shows no significant linear relationship between stress and strain (Wu and Song, 2022). Therefore, an effective simulation model to characterize the physical properties of kiwifruit stalks is essential for the development of machinery equipment aimed at enhancing post-harvest kiwifruit quality (Li *et al*., 2020).

In recent years, the discrete element method has been widely used in the field of agricultural engineering as a numerical simulation and analysis method that reveals the relationship between the actions of crops and their mechanical structure (Zeng *et al*., 2021; Kafashan *et al*., 2021). Researchers have conducted discrete element numerical simulations of flexible stems, including corn (Leblicq *et al*., 2016b; Zhang *et al*., 2023; Fang *et al*., 2022), alfalfa (Ma *et al*., 2022)., and rape stalks (Liao *et al*., 2020)., and the results have shown that the model parameters vary significantly for different stalks. The construction of a discrete element model of a stem requires a combination of intrinsic material, contact, and bond parameters (Li *et al*., 2023). The stem mechanical properties and contact parameters can be directly calculated; however, the bond parameters are difficult to obtain using direct instrumental measurements(Zhang *et al*., 2020; Horabik *et al*., 2022). Therefore, it was necessary to calibrate the bonding parameters using mechanical tests. As intelligent agricultural equipment develops toward informatization and intelligentization, higher demands are imposed on harvesting robot end effectors that are in direct contact with fruits (Zhang *et al*., 2020). The discrete element bonding model based on Hertz-Mindlin with bonding can effectively characterize the physical properties of the material and reveal the mechanism of action between the agricultural crop and mechanical equipment (Liu *et al*., 2022; Wang *et al*., 2022; Wang *et al*., 2021; Ucgul *et al*., 2017). The stability of the discrete element model simulation depends on the simulation parameters (Schramm *et al*., 2022). Therefore, the calibration of the discrete element model parameters is essential. The establishment of an accurate discrete element model of the kiwifruit stalk enables the analysis of the mechanism of the interaction between the stalk and the contact structure, guiding the design and simulation optimization of the end-effector.

The discrete element method (DEM) exhibits remarkable performance in microstructural analysis, particularly in its suitability for simulating stem materials (Wu and Song, 2022). DEM accurately analyzes inter-particle interactions, allowing for a more detailed analysis compared to the finite element method (Zeng *et al*., 2021). Stem fibers, featuring cohesive forces, align well with DEM's resolution of intermolecular interaction (Sadrmanesh *et al*., 2021; Sadek *et al*., 2011), making it highly suitable for examining stem material behavior at the granular level. DEM excels in simulating discontinuities and fractures, enabling more precise modeling of fiber fracture or debonding processes (Chen *et al*., 2014). It offers simpler parameterization, especially concerning discrete particles. Concerning complex mixed material systems in agriculture, DEM efficiently models interaction mechanisms between different components (Zhang *et al*., 2023), thereby laying essential theoretical groundwork for addressing vibration and damage concerns in robotic harvesting.

There are no published studies on the calibration of discrete element model simulation parameters for kiwifruit stalk. In this study, the Hertz-Mindlin with bonding contact model was adopted as the discrete element model for kiwifruit stalks with its intrinsic and contact parameters, which were calibrated using three-point bending tests and shear tests. The fruit stalk bending and shear mechanical tests were simulated using the discrete element mode, and the reliability of the calibrated bonding model was verified by comparing it with actual mechanical tests of the fruit stalks.

Materials and Methods

Experimental materials

The test material for this study was Hayward kiwifruit stalks obtained from the Kiwifruit Experiment Station of Northwest Agriculture and Forestry University. The test samples were collected during the 2022 kiwifruit harvest season, and 100 kiwifruit stalks were randomly obtained to ensure stalk variability. The diameter and length were measured using a Vernier caliper with an accuracy of 0.01 mm. The statistical analysis in Figure 1 revealed an average diameter of 3.68 mm and an average length of 43.84 mm of kiwifruit stalks. The moisture content of all samples was between 39.5% and 46%, and to ensure the accuracy of the test results, the mechanical tests were completed within 24 h.

Discrete element model of kiwifruit stem

The discrete element model of the stem is composed of a plurality of particles with interparticle bonding to characterize mutual interactions. To accurately simulate the mechanical properties of kiwifruit stalks in bending and shear, the Hertz-Mindlin bonding contact model was used for the simulation. As shown in Figure 2, the material mechanical properties are represented by the forces and torques of the interparticle contact (Wang *et al*., 2020) and are calculated using the following relationship:

$$\begin{cases} \delta F_b^n = -v_n k_n A \delta_t \\ \delta F_b^t = -v_t k_t A \delta_t \\ \delta M_b^n = -\omega_n k_t J \delta_t \\ \delta M_b^t = -\omega_t k_n J \delta_t / 2 \end{cases} \quad (1)$$

where δF^n_b is normal bonding force (N), δF^t_b is shear bonding force (N), δM^n_b is normal moment (N/m), δM^t_b is shear moment (N/m), v_n is normal velocity (m/s), v_t is tangential velocity (m/s),

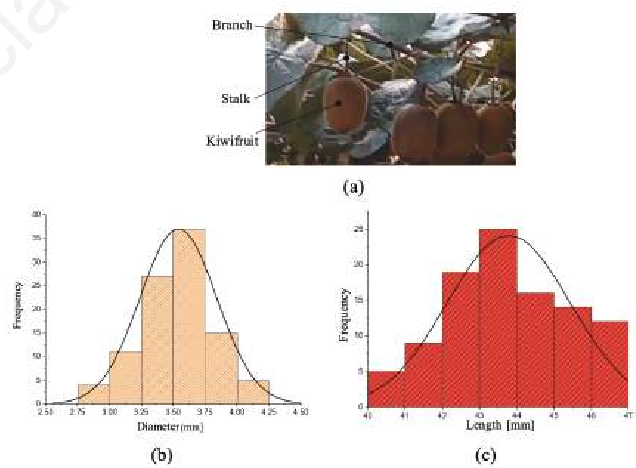

Figure 1. Size distribution of kiwifruit stalks.

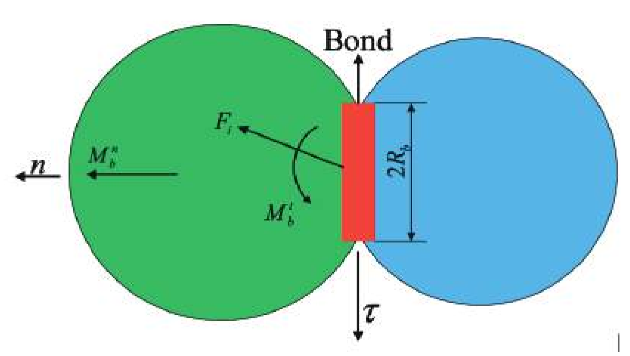

Figure 2. Hertz-Mindlin model with the bonding contact.

w_n is the normal angular velocity (rad/s), w_t is the shear angular velocity (rad/s), k_n is normal stiffness (N/m^3), k_t is the shear stiffness (N/m^3), d_t is the time step (s), A is the contact area (m^2), J the is rotational inertia (m^4).

The bond fractures as the forces between the particles exceed the critical normal and shear stresses (Zhao *et al.*, 2023). Therefore, the mechanical properties of kiwifruit stalks were numerically simulated using bond fracture. The normal and shear critical stresses were calculated as follows:

$$\sigma_{\max} < \frac{-F_n}{A} + \frac{2M_b^t}{J} R_b$$
$$\tau_{\max} < \frac{-F_t}{A} + \frac{2M_b^n}{J} R_b \quad (2)$$

where σ_{max} is the critical normal stress (Pa), t_{max} is the critical shear stress (Pa), R_b is the bonded radius (mm).

Obtaining the parameters of the discrete element model of the kiwifruit stem

Determining the intrinsic parameters

Density: the intrinsic parameters of kiwifruit pedicel materials include density, Poisson's ratio, and modulus of elasticity. The drainage method (Zhang *et al.*, 2023) is widely employed for density measurements in the parameter assessment of discrete element method simulations. The density was calculated using the following equation:

$$\rho = \frac{m}{V} \quad (3)$$

where m is the mass (g), V is the volume (cm^3).
The sample volume was measured by the drainage method, and the sample mass was weighed with an electronic scale of 0.01 g accuracy.

Poisson's ratio: as a coefficient of transverse deformation reflecting unidirectional tension and compression of the material, it was calculated as follows:

$$\varepsilon = \left|\frac{\Delta\delta_1}{\Delta\delta_2}\right| \quad (4)$$

where $\Delta\delta_1$ is lateral deformation (mm), $\Delta\delta_2$ is longitudinal deformation (mm).

Elastic modulus: when a material undergoes elastic deformation, the material stress is proportional to the strain; thus, the modulus of elasticity was calculated by the formula.

$$E = \frac{F_1 / S}{\Delta L / L} \quad (5)$$

where F_1 is the load (N), S is the cross-sectional area of stalk (m^2), DL is the tensile elongation (mm), L is the initial length of stalk (mm). The Poisson's ratio and elastic modulus were measured with a texture analyzer (Universal TA, Teng Dial Instruments, Shanghai, China). As shown in Figure 3, a tensile test was performed on a randomly selected kiwifruit pedicel using a texture analyzer at a loading speed of 2 mm/min. The parameters of the kiwifruit stalks were measured according to Poisson's ratio. The original length and tensile extension of kiwifruit stalks were measured with an accuracy of 0.02 mm vernier caliper. Determining the elastic modulus involves three primary steps. First, a 2 cm segment from the midsection of the kiwifruit pedicel was chosen as the experimental sample. Second, both ends of the pedicel were securely fixed onto the A/TG probe, preceded by three preliminary trials to ensure a non-slip process during loading at a rate of 6 mm/min for 2 seconds. Finally, the pedicel underwent tensile testing at a loading rate of 2 mm/min until fracture, concluding the experiment. Instances of slippage or rupture at the clamping sites during the test were deemed failures and excluded from the calculation of the elastic modulus.

Determining the contact parameters

Restitution coefficient

A free-fall test was used to measure the restitution coefficient between the kiwifruit stalk and the steel components (Figure 4). The measured material was dropped from the height, contacted with the steel parts, and bounced upward by collision. The experimental process comprised the following steps: i) setting coordinate board values on the tabletop; ii) raising individual stalks to a fixed height, allowing them to fall freely from rest, recording their rebound height upon collision with a rigid board; and iii) the maximum height of the kiwifruit stalk at the rebound stage was captured using a high-speed camera (i-SPEED; Olympus Co., Ltd., Tokyo, Japan). Rebound heights were calculated using coordinate paper with a minimum measurement unit of 1 mm. The restitution coefficient was calculated as follows:

$$e = \frac{I_2}{I_1} = \frac{v_2}{v_1} = \sqrt{\frac{2gH_2}{2gH_1}} = \sqrt{\frac{H_2}{H_1}} \quad (6)$$

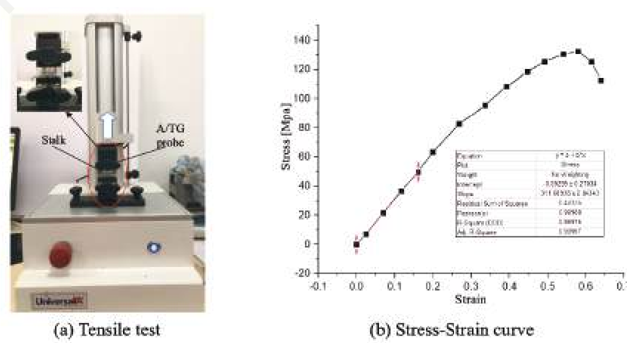

Figure 3. Tensile test of kiwifruit stalk.

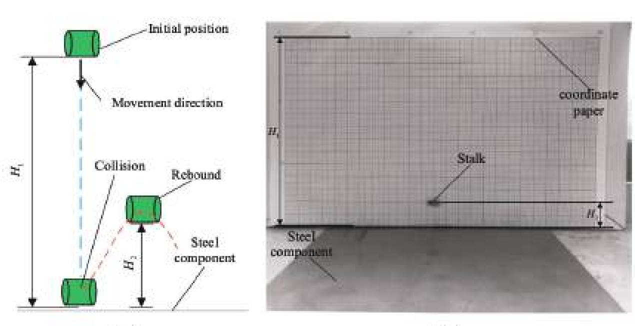

Figure 4. Measurement of the restoration coefficient between kiwifruit stalks and steel components.

where e is the restitution coefficient, I_1 is the pre-collision impulse (N×s), I_2 is the post-collision impulse (N×s).

Static friction coefficient and rolling friction coefficient

The static and dynamic friction coefficients of kiwifruit stalks against steel parts were measured using the inclined-plane method (Ding *et al*., 2022; Horabik *et al*., 2016). The measurement principle is illustrated in Figure 5a. With an increase in the angle of inclination between the steel parts and the horizontal surface, the fruit stalk gradually moved, and the static friction coefficient was calculated as follows:

$$\mu_f = \tan\theta \tag{7}$$

where θ is the tilting angle. As shown in Figure 5b, the kiwifruit stalk undergoes rolling movement at an angle of inclination greater than the critical angle, and the kiwifruit stalk rolls freely from the initial position without an initial velocity along the inclined plane to the end position. Assuming that the kiwifruit stalk is subjected to friction only during the rolling process, the coefficient of kinetic friction between the kiwifruit stalk and the steel part was calculated according to the law of conservation of energy.

$$mgL_1 \sin\beta = mg(L_1 \cos\beta + L_2)\mu_s \tag{8}$$

where L_1 is the distance travelled along the inclined plane (mm), L_2 is the distance travelled along the plane (mm).

Calibration method for kiwifruit stalk DE model

The bonding model is effective for characterizing the physical properties of a material (Leblicq *et al*., 2016a). Bending strength and shear force are significant mechanical parameters for characterizing the stalk cutting process and are closely related to their material properties (Jiang *et al*., 2021). Therefore, this mechanical parameter can be applied to the calibration of the discrete element bonding parameters of the kiwifruit stalk.

Three-point bending test

Experiments and simulations were conducted to determine the optimal combination of parameters between the normal stiffness k_n, shear stiffness k_t, and bond radius R_j for kiwifruit stalks. The test was designed by combining the results of the three-point bending simulation test with bending strength as the test indicator. The test factors are k_n, k_t, and R_j. A regression model was established between the test factors and test indices using a quadratic fitting equation to analyze the influence of the test factors and indices. The minimum relative error between the simulation and real values of three-point bending.

The optimal combination of parameters was calibrated and solved as follows: i) a three-point bending test was designed to calculate the bending strength of the kiwifruit pedicel; ii) a three-point bending simulation test of the kiwifruit stalk was devised and the relevant parameters were set; and iii) response surface method tests were developed to establish parametric regression equations between the normal stiffness, tangential stiffness, bond radius, and bending strength of kiwifruit stalks, and optimized solutions were obtained.

Bending strength defines the maximum stress a material endures before fracturing under bending loads, indicating the pedicel's ability to resist bending. The three-point bending test restricts the stem with four degrees of freedom and applies force through a probe until failure transpires. Assumptions in computing bending strength follow the plane stress hypothesis, assuming the material's cross-section remains planar and perpendicular to the axis post-bending deformation. The bending strength was calculated as:

$$\sigma_c = \frac{M_{\max}}{W} = \frac{FL_3/4}{\pi D^3/32} = \frac{8FL_3}{\pi D^3} \tag{9}$$

where M_{max} is the maximum bending moment, W is the section modulus in bending, F is the bending force (N), L_3 is the support distance (mm), D is the stalk diameter (mm).

Shearing test

The normal critical stress $\sigma_{\max}$ and the shear critical stress t_{max} were calibrated using a combination of shear tests and simulations. The regression fitting model between the fruit stalk shear force F_c and test factors $\sigma_{\max}$ and t_{max} was established using F_c in the simulation test as the test index. Optimized solution with the minimum relative error between the simulated and real values of the shear test. The calibration solution steps were as follows: i) a shear test was designed to calculate the average shear force on the kiwifruit stalk; ii) a three-point bending simulation test was devised to determine the optimal interval between normal critical stress and shear stress using a numerical comparison method; and iii) a parametric regression model was developed to optimize the calibration parameters and obtain the optimal bonding parameter values.

Results

Calibration results for normal stiffness, shear stiffness, and bonded disk radius

Three-point bending test analysis

A three-point bending test was performed on kiwifruit stalks using a Universal TA texture analyzer (Figure 6) with a three-point

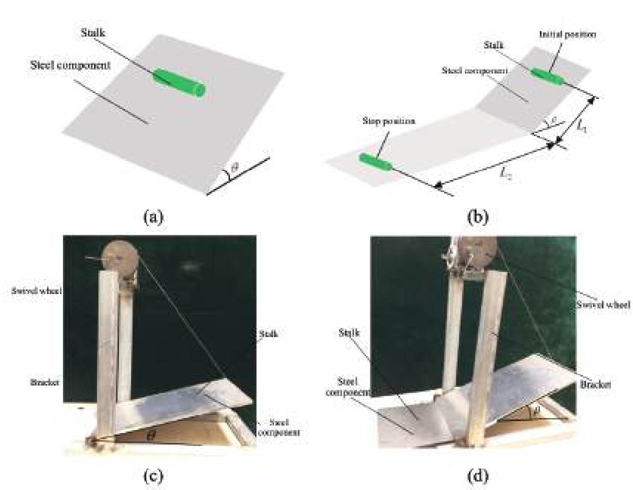

Figure 5. Principle diagram of friction coefficient measurement.

bending indenter type P/3PB, a loading speed of 2 mm/s, and loading time of 3 s. The force-displacement curves of the kiwifruit stalks were obtained from the test and the maximum bending force (F) applied to the kiwifruit stalks in the bending test was recorded. The bending strength (σ_c) of kiwifruit stalks was calculated according to the force-time curves. From the measurements of 20 kiwifruit stalks (Table 1), the average value of the bending strength was calculated as 6.75 MPa in combination with Eq. (6), and this value was used as the response value in the simulation analysis.

Simulation model and parameter settings

The kiwifruit stalk three-point bending simulation test (Figure 7) utilized the Hertz-Mindlin with bonding model in the EDEM software to characterize the physical properties of the material. To reduce computational load, a discrete element model of kiwifruit stalks was developed using particle stacking. Because no fracture occurred in the kiwifruit stalk during the simulation, σ_{max} and t_{max} were set to 1×10^7 Pa regarding the parameters of the flexible stalk. The simulation model parameters were determined as listed in Table 2 by combining the intrinsic and contact parameters obtained from physical experiments. Twenty kiwifruit stems were selected as experimental samples for each set of parameter measurements. Due to the utilization of the drainage method for measuring pedicel density, an assessment was conducted for the moisture content before and after measurement. The results indicate a moisture content variation of 0.32-0.65% before and after measurement.

Response surface test analysis

The response surface method was used to calibrate three parameters: normal stiffness, tangential stiffness, and bond radius. The bending strength σc in the simulation test was used as the test evaluation index, and the normal stiffness k_n, tangential stiffness k_t, and bond radius R_j were analyzed. The control factors and their levels were determined through a stimulation pretest, as shown in Table 3. Quadratic regression equations for the evaluation indices and test factors were established using Design-Expert software with the experimental design scheme, and the results are shown in Table 4. The regression equation is as follows:

$$\sigma_c = 5.96 + 4.51k_n + 2.03k_t + 1.39R_j + 2.13k_nk_t + 1.25k_nR_j + 0.52k_tR_j - 0.4943k_n^2 - 1.38k_t^2 - 0.0543R_j^2$$

The analysis of variance ANOVA of the test results is shown in Table 5, where the p-value (model) is <0.0001, indicating a significant effect of the model. The p-value (lack of fit) was >0.05, indicating a high fit for the regression equation and statistical validation of the model. k_tR_j, $k_{n,}{}^{2}$, and R_j^2 were irrelevant to the model (p>0.05), whereas the other test factors indicated a significant effect (p<0.05) on the bending strength model. The response surface analysis of the three parameters is shown in Figure 8.

Determination of optimal parameter combinations

The relative error between the measured bending strength σ_c' and the simulated value σ_c in the three-point bending test was used as an index to determine the optimal combination. The relative error was calculated as follows:

$$\eta = \frac{|\sigma_c - \sigma_c'|}{\sigma_c'} \tag{10}$$

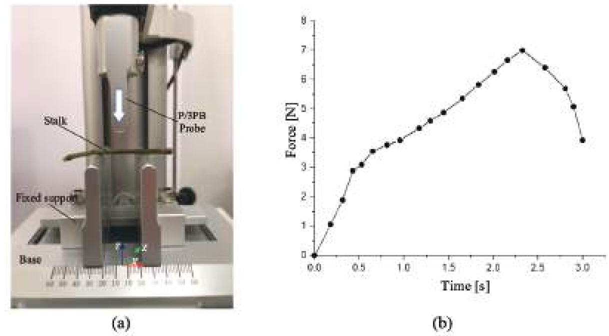

Figure 6. Three-point bending experiment.

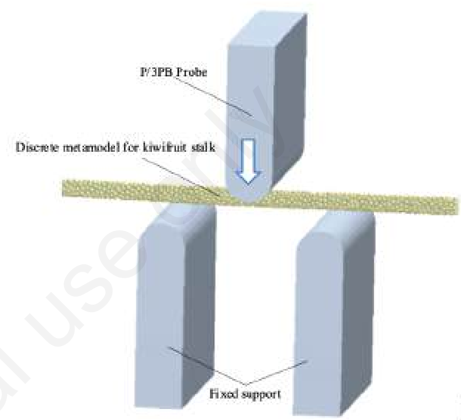

Figure 7. Three-point bending simulation experiment.

Table 1. Results of three-point bending tests of kiwifruit stalks.

Test number	F (N)	σc (MPa)
1	3.48	5.58
2	3.58	6.01
3	4.28	7.51
4	3.95	6.99
5	4.52	7.99
6	4.19	7.22
7	3.68	6.36
8	3.23	5.52
9	4.48	7.82
10	3.61	6.27
11	3.58	6.05
12	3.51	5.66
13	3.62	6.41
14	3.29	5.59
15	3.91	6.92
16	3.62	6.82
17	4.52	7.92
18	4.38	7.76
19	4.15	7.18
20	4.25	7.46
Average	3.89	6.75
Standard deviation	0.412	0.824

With the relative error as the response value, the response surface method was used to search for the optimal combination of normal stiffness, shear stiffness, and bond radius parameters. The optimization constraints were set as follows:

$$\begin{cases} \min \eta\left(\sigma_c, \sigma_c^{'}\right) \\ s.t. \begin{cases} -1 \le k_n \le 1 \\ -1 \le k_t \le 1 \\ -1 \le R_j \le 1 \end{cases} \end{cases} \tag{11}$$

The optimal three-parameter combinations were determined based on the optimized conditions and response values. The results indicated a normal stiffness k_n of 7.201×10^{11} N/m^3, shear stiffness k_t of 2.379×10^{11} N/m^3, and bond radius R_j of 0.164 mm.

Calibration results for the critical normal stress and critical shear stress

Shearing test analysis

Shear tests on fruit stalks were performed using a Universal TA texture analyzer (Figure 9). The cutter type was P/MORS, loading speed was 2 mm/s, and loading time was 3 s. The force-displacement curve of the Kiwifruit stalks was obtained and the maximum shear force on the stalks during the shear test was recorded. According to the results of the 20 kiwifruit stalk shear tests, the average shear force of the kiwifruit stalks was calculated to be 8.62 N.

Kiwifruit stalk shear simulation test

By combining the kiwifruit stalk simulation model parameters (Table 2) and calibrated parameters, shear simulation tests were performed using EDEM software, as shown in Figure 10. The shear force of kiwifruit stalks after breakage was recorded in the simulation tests. The shear simulation tests were analyzed by setting different σ_{max} and t_{max} values to obtain the shear force varia-

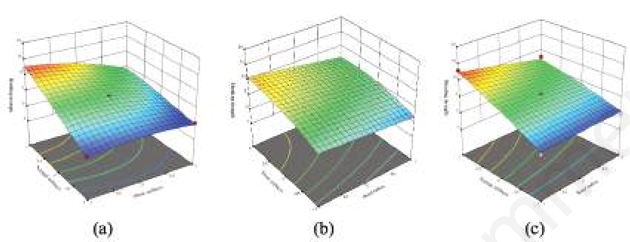

Figure 8. Response surface analysis.

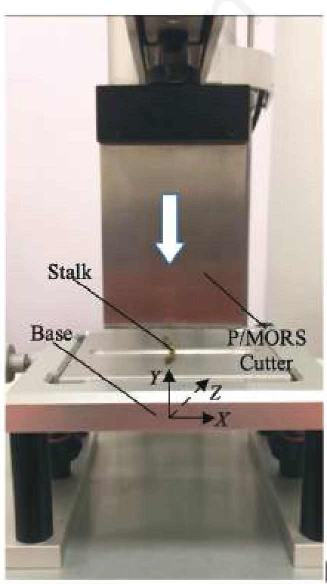

Figure 9. Kiwifruit stalk shear test.

Table 2. Parameters of discrete element model for three-point bending test.

Parameters	Value	Standard deviation
Density of kiwifruit stalk (kg/m^3)	867.5	1.785
Density of steel component (kg/m^3)	7.85×10^3	2.142
Poisson's ratio of kiwifruit stalk	0.26	1.953
Poisson's ratio of steel component	0.30	2.014
Elastic modulus of kiwifruit stalk (Pa)	3.25×10^8	1.596
Elastic modulus of steel component (Pa)	2.06×10^{11}	1.423
Restitution coefficient	0.365	2.234
Static friction coefficient	0.152	2.342
Rolling friction coefficient	0.08	1.915

Table 3. Coded parameters levels.

Parameters	k_n (N*m^{-3})	k_t (N*m^{-3})	R_j (mm)
-1	5×10^9	5×10^9	0.155
0	4.525×10^{11}	2.525×10^{11}	0.185
1	9×10^{11}	5×10^{11}	0.215

Table 4. Experiment analysis scheme and test results.

PNo.	Test factors			Evaluation index
	k_n	k_t	R_j	σ_c
1	-1	-1	0	0.22
2	1	-1	0	3.63
3	-1	1	0	0.28
4	1	1	0	12.21
5	-1	0	-1	0.16
6	1	0	-1	8.02
7	-1	0	1	0.29
8	1	0	1	13.16
9	0	-1	-1	1.68
10	0	1	-1	4.43
11	0	-1	1	3.58
12	0	1	1	8.41
13	0	0	0	5.96
14	0	0	0	5.91
15	0	0	0	5.98
16	0	0	0	5.96
17	0	0	0	5.97

tion patterns of kiwifruit stalks under different conditions to determine the optimal value intervals for each factor. The results are shown in Figure 11. The fracture between the cutting knife and kiwifruit stalk model occurred with only contact, as the critical stresses σ_{max} and t_{max} were 1×10^6 Pa. As the critical stress increases, the shear force changes significantly. After exceeding the range of 1×10^{10} Pa, the shear force changed gradually and smoothly, indicating that the critical stress range was within this interval after calibration of the three parameters.

Parameter optimization

A regression fitting method was used to calibrate the two parameters of normal critical stress σ_{max} and shear critical stress t_{max}. The shear force F_c in the simulation experiment was used as the response value, and σ_{max} and t_{max} were the test factors for the analysis. Combined with the optimal value interval determined in the simulation test, the control factors and levels were determined as listed in Table 6. The regressions of the shear force were fitted in different ways and combined with the experimental results as shown in Table 7.

The regression fitting results are shown in Table 8, where the determination (R^2) is -3.393×10^{17} and the sum of squares (SSE) is 3.072×10^{17}, indicating that the interaction-type regression model has an insignificant fitting ability and does not have an excellent predictive effect. The determination (R^2) of the quadratic polynomial regression model was 0.9994 and the sum of squares (SSE) was 0.05003. Compared with the three regression models, such as linear and quadratic interactions (Figure 12), the quadratic regression model has higher reliability and good predictive performance. The quadratic regression equation is as follows:

$$F_c=2.241+6.562e^{-11}\sigma_{max}+3.642e^{-09}\tau_{max}+3.178e^{-20}\sigma_{max}\tau_{max}-1.617e^{-20}\sigma_{max}^{2}+-3.824e^{-19}\tau_{max}^{2}$$

The analysis of the variance of the test results are shown in Table 9, and the model was in the extremely significant difference state, indicating that the regression equation had a high degree of fitting, indicating the regression equation was highly fitted. The effect of the shear model was highly significant for the critical normal stress and insignificant for the critical shear stress.The parameters were calibrated using a quadratic polynomial regression model with the average shear force as the response value in the shear test. The results showed a σ_{max} of 5.937×10^8 Pa and t_{max} of 2.354×10^9 Pa. A shear force of 8.772N with a relative error of 1.76% was obtained when the parameters were introduced into the

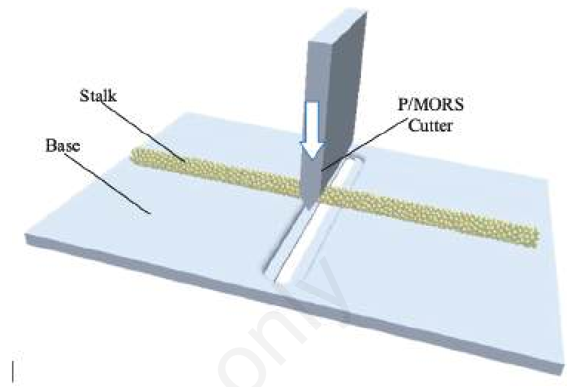

Figure 10. Shear test simulation test.

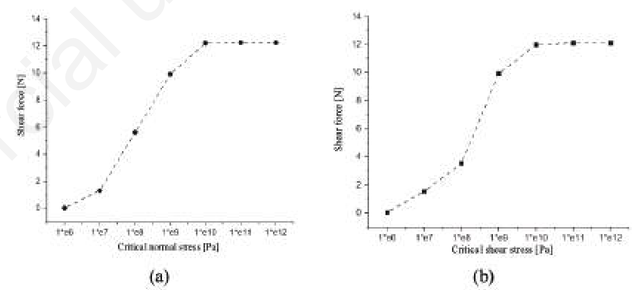

Figure 11. Effect of critical stress on shear.

Table 5. Analysis of variance for the three-point bending test.

Source	Bending strength σ_c			
	Sum of squares	DOF	F-value	p
Model	246.00	9	50.07	<0.0001**
K_n	162.63	1	297.91	<0.0001**
K_t	32.89	1	60.24	0.0001**
R_j	15.54	1	28.47	0.0011**
$K_n K_t$	18.15	1	33.24	0.0007**
$Kn Rj$	6.28	1	11.49	0.0116*
$K_t R_j$	1.08	1	1.98	0.2021
Kn_2	1.03	1	1.88	0.2122
K_t^2	7.98	1	14.62	0.0065**
R_j^2	0.0124	1	0.0227	0.8845
Residual	3.82	7	0.5459	
Lack of fit	3.82	3	1.27	<0.0001**
Pure error	0.0029	4	0.0007	
Cor total	249.86	16		

regression equation. The results indicate that the shear regression equation has excellent reliability.

Analysis and verification test

To further verify the reliability of the model simulation parameters, an equivalent model of the kiwifruit pedicel was established based on the calibration parameters, and three-point bending and shear simulation tests were performed using EDEM software. The study conducted simulations employing the EDEM 2020 software on a computational system comprising 32GB of RAM, an NVIDIA GeForce RTX 3060 GPU, an i7-11700K CPU, and 32GB of memory. Simulation settings were adjusted to align with the parameters employed in the three-point bending experimental tests, ensuring consistency. The simulation results were compared with those of the five test sets. The average bending strength of the five sets of tests was 7.04 Mpa and the average shear force was 8.53 N. The simulations resulted in a bending strength of 6.89 Mpa and a shear force of 8.86 N. The relative errors between the measured values were 2.13% and 2.84%, respectively. A comparison with actual tests (Figures 13-14) shows that the discrete element equivalent model can characterize the physical properties of kiwifruit stalks

Table 6. Coded shear test parameter levels.

Parameters	σ_{max} (Pa)	τ_{max} (Pa)
-1	5×10^8	5×10^8
0	1.5×10^9	3×10^9
1	5.5×10^9	5×10^9

Table 7. Shear test analysis scheme and test results.

σ_{max} (Pa)	τ_{max} (Pa)	F_c (N)
5×10^8	5×10^8	4.03
	3×10^9	9.88
	5×10^9	10.89
1.5×10^9	5×10^8	3.96
	3×10^9	9.96
	5×10^9	11.25
5.5×10^9	5×10^8	3.99
	3×10^9	10.01
	5×10^9	11.68

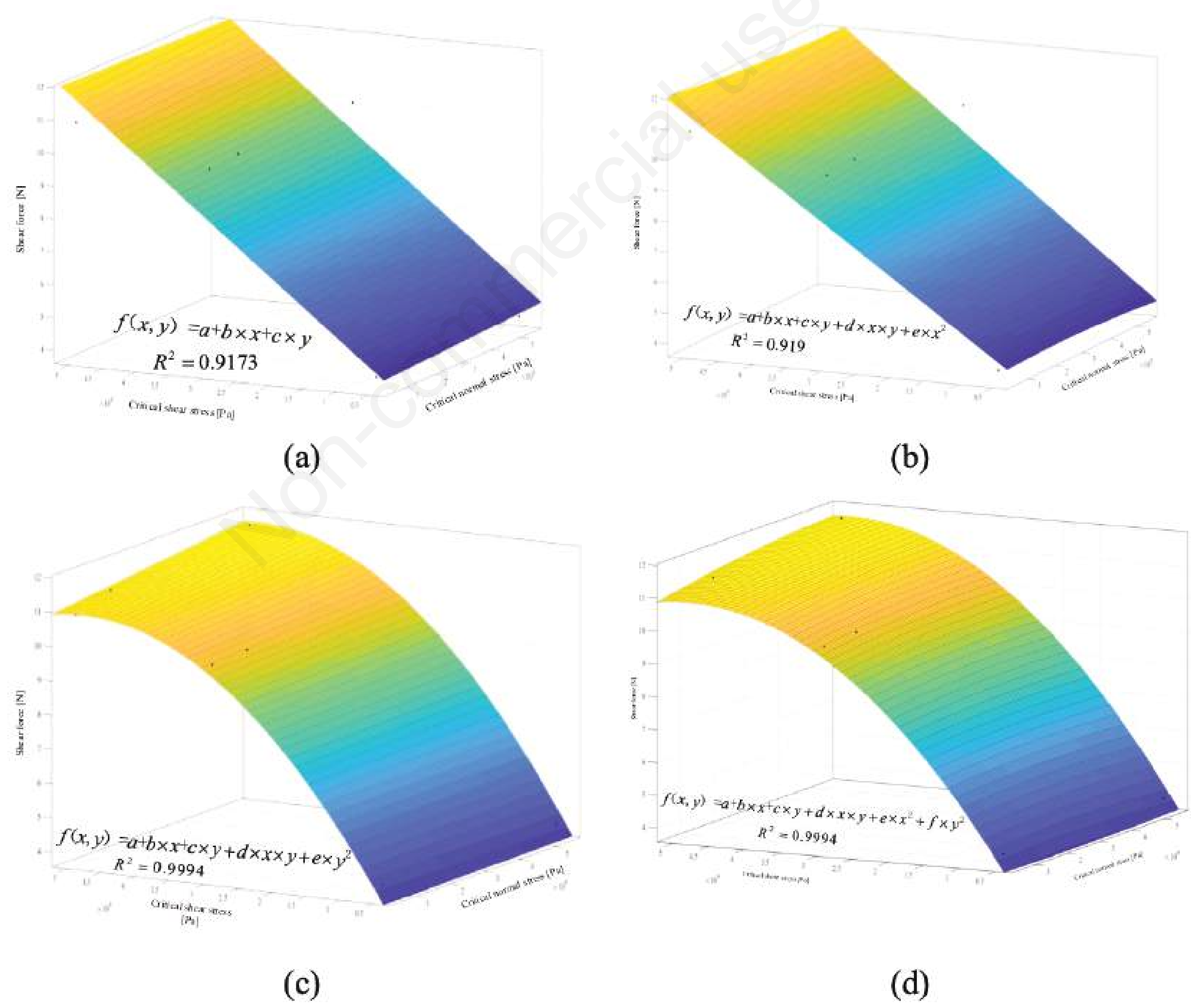

Figure 12. Schematic of regression fitting equation.

with accurate calibration parameters. The results of the kiwifruit stalk shear test and the simulation are compared in Figure 15. A comparative analysis shows that the relationship between the shear force and displacement obtained from the simulation exhibits the same trend as that of the actual test. The shear force increased with displacement until the separation of the stalk occurred at the maximum shear force. The maximum shear forces for the five sets of shear tests were 8.93 N, 8.80 N, 8.41 N, 8.30 N, and 8.21 N, respectively, whereas the simulation values were 8.86 N with relative deviations of 1.35%, 1.80%, 6.32%, 3.95%, and 7.90 %, respectively. The results show that the parameter-calibrated discrete element model can reflect the force-displacement relationship in the shearing process of kiwifruit stalks.

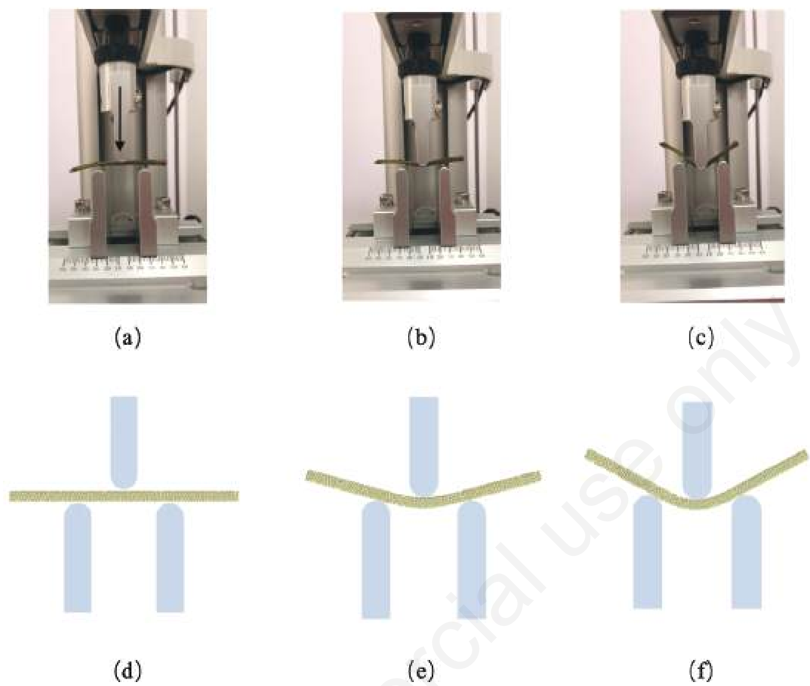

Figure 13. Kiwifruit stalk three-point bending verification test..

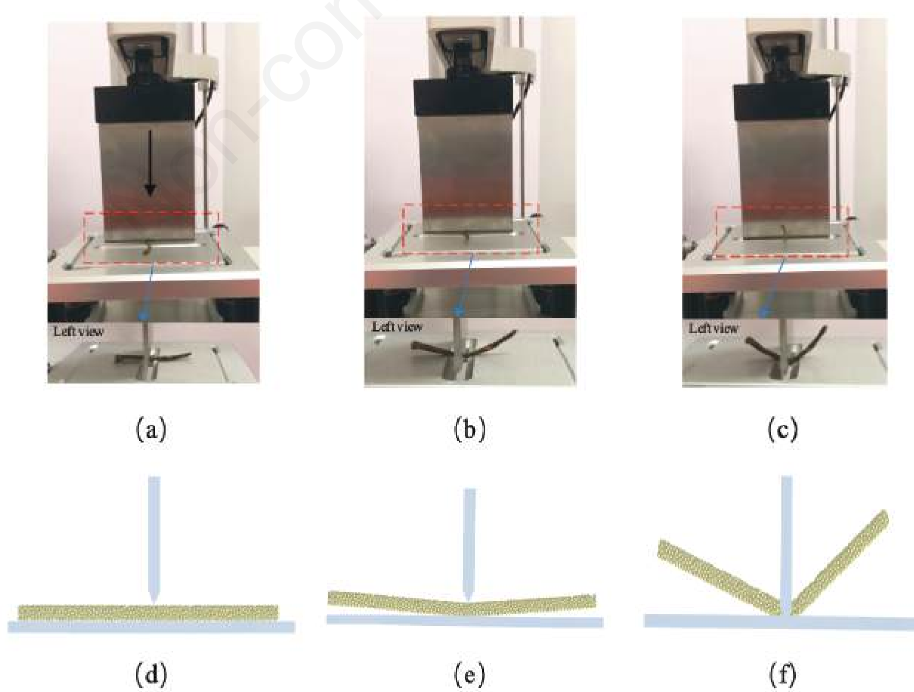

Figure 14. Kiwifruit stalk shear validation test.

Discussion

In this study, a discrete element model with the Hertz-Mindlin with bonding model was applied to the kiwifruit stalk, and the reliability of the model was verified by mechanical tests. The established discrete element model can accurately characterize the mechanical properties of kiwifruit stalks during bending and shearing; however, the force-displacement curves obtained by simulation in the EDEM were different from the mechanical test results. Although there were some discrepancies between the force and displacement curves during the simulation and the actual shear test, the maximum shear force, and curve variation trends were the same as the actual values. In addition, the shear test revealed the presence of the next maximum peak after the maximum shear force. The test was conducted under observation. First, it was discovered that the maximum shear force failed to completely cut off the fruit stalks and that the internal tissues of the fruit stalks existed based on the connection relationship. Second, the maximum shear force was followed by a reduction in the stiffness of the fruit stalk, leading to a reduction in the next peak shear force, which separated the stalk with continuous tool motion. The model constructed in this study was unable to effectively reflect the force-displacement curve at the stage after the maximum shear, and the next stage of the study attempted to construct a discrete element model from the discrete element particle accumulation mode and the analysis of the internal components of the stalk. In addition, stalks with different moisture content exhibited different maximum shear forces, and the moisture content of the experimental material during the test process was strictly ensured. Throughout the experiment, the moisture content of the samples ranged from 39.5% to 46%. Notably, samples from test 3 and test 5 exhibited the largest deviations from the simulation models, with moisture contents of 45.5% and 44.6%, respectively. The moisture content in the remaining three sets fell within the 41.5% to 43% range. These findings underscore the pivotal role of moisture content as a significant factor impacting stems shear tests. Future simulations will encompass additional considerations, including kiwifruit pedicel varieties, diameters, and location-specific moisture levels during shearing. This comprehensive approach aims to precisely characterize the mechanical properties of kiwifruit pedicels under diverse conditions.

Although the discrete element model constructed in this study failed to fully reflect the biomechanical properties of kiwifruit stalks, it was sufficient for the design and development of shear mechanical structures, particularly kiwifruit picking end-effectors. In addition, a subsequent study considered the maximum shear force as the response value and optimal parameters of the shearing mechanism to predict the shearing effect of different mechanical structures via simulation.

Conclusions

Experiments and simulations were conducted on the kiwifruit stalks. The intrinsic and contact parameters of the stalk were experimentally tested. Based on this a discrete element model of kiwifruit stalks was constructed. Three-point bending and shear simulation tests of the discrete element model were performed using the EDEM software, with bending strength and shear as response values, to calibrate the bonding parameters. The optimal bonding parameters were: $k_n = 7.201\times10^{11}$ N/m^3, $k_t = 2.379\times10^{11}$ N/m^3, $R_j = 0.164$ mm, $\sigma_{max} = 5.937\times10^8$ Pa, and $t_{max}=2.354\times10^9$ Pa. The calibrated discrete element model was validated through mechanical tests, and the results showed that the discrete element equivalent model of the kiwifruit stalk was capable of effectively characterizing its physical properties. Compared with the mechanically realized results, the relative error ratios for the bending

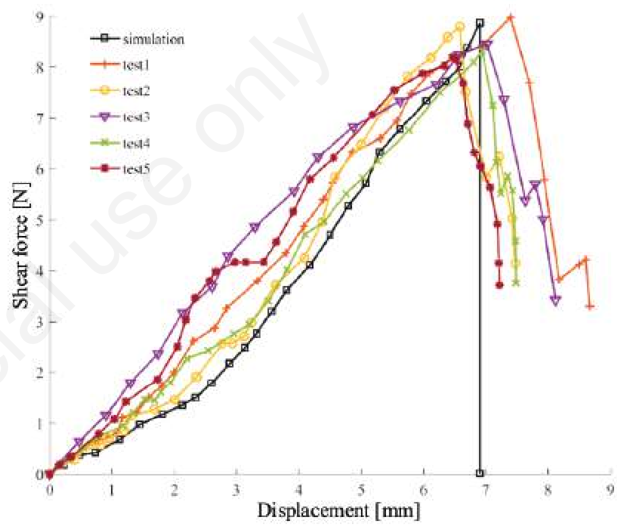

Figure 15. Shear test force-displacement curves..

Table 8. Regression fitting results.

Regression model	Regression equation	R^2	SSE	Adjusted R^2
Linear	$f(x, y) = a+bx+cy$	0.9173	7.484	0.8898
Interaction	$f(x, y) = a+bx+cy+dxy$	$-3.393e^{+17}$	$3.072e^{+19}$	$-5.428e^{+17}$
Quadratic polynomial interaction-type	$f(x, y) = a+bx+cy+dxy+ex^2$	0.919	7.333	0.838
Quadratic polynomial interaction-type	$f(x, y) = a+bx+cy+dxy+ey^2$	0.9994	0.05749	0.9987
Quadratic polynomial	$f(x, y) = a+bx+cy+dxy+ex^2+fy^2$	0.9994	0.05003	0.9985

Table 9. Analysis of variance for shear tests.

Source	Shearing force			
	Sum of squares	DOF	F-value	p
Model	90.3616	4	466.3158	<0.0001**
σ_{max}	0.1301	2	1.3433	0.3579
τ_{max}	90.2315	2	931.2888	<0.0001**
Pure error	0.19378	4		
Cor total	90.5554	8		

strength and shear were 2.13% and 2.84%, respectively, indicating that the calibration parameters were reasonable. These results can be used as a theoretical basis for the structural optimization of fruit stalk-cutting machinery at a later stage. Future research endeavors will concentrate on enhancing the calibration of stem discrete element model parameters. We aim to explore the utilization of machine learning to improve the precision of model parameter calibration, thereby enhancing the representation of material mechanical properties.

References

Chen, Y., Sadek, M.A., Guzman, L. Lague, C., Landry, H. 2014. Simulation of tensile tests of hemp fibre using discrete element method. CIGR J. 16:126-135.

Ding, X.T., Li, K., Hao, W., Yang, Q.C., Yan, F.X., Cui, Y.J. 2023. Calibration of simulation parameters of camellia oleifera seeds based on RSM and GA-BP-GA optimization. Trans. Chinese Soc. Agric Mach. 54:139-150.

Ding, X.T, Wang B.B, He, Z, Yang, Q.C., Cui, Y.J. 2023. Fast and precise DEM parameter calibration for Cucurbita ficifolia seeds. Biosyst. Eng. 236:258-276.

Fang, M., Yu, Z., Zhang, W., Cao, J., Liu, W., 2022. Friction coefficient calibration of corn stalk particle mixtures using Plackett-Burman design and response surface methodology. Powder Technol. 396:731-742.

He, Z., Ma L., Wang Y.C., Wei, Y.Z., Ding, X.T., Li, K., Cui, Y.J 2022. Double-arm cooperation and implementing for harvesting kiwifruit. Agriculture (Basel) 12:1763

Horabik, J., Molenda, M., 2016. Parameters and contact models for DEM simulations of agricultural granular materials: A review. Biosyst. Eng. 147:206-225.

Jiang, P., Li, Y., Li, J., Meng, H., Peng, X., Zhang, B., et al. 2021. Experimental research on the bending and fracture characteristics of cotton stalk. Trans. ASABE 64:1771-1779.

Kafashan, J., Wiacek, J., Ramon, H., Mouazen, A.M., 2021. Modelling and simulation of fruit drop tests by discrete element method. Biosyst. Eng. 212:228-240.

Liao, Y.T, Liao, Q.X, Zhou Y., Wang, Z.T., Jiang, Y.J., Liang F. 2020. Parameters calibration of discrete element model of fodderrape crop harvest in bolting stage. Trans. Chin. Soc. Agric. Machin. 51:73-82.

Li, J., Lu, Y., Peng, X., Jiang, P., Zhang, B., Zhang, L., et al. 2023. Discrete element method for simulation and calibration of cotton stalk contact parameters. Bioresources 18:400-416.

Liu, Y., Zhao, J., Yin, B., Ma, Z., Hao, J., Yang, X., et al. 2022. Discrete element modelling of the yam root-soil complex and its verification. Biosyst. Eng. 220:55-72.

Li, J., Liu, X., Zou, L., Yuan, J., Du, S., 2020. Analysis of the interaction between end-effectors, soil and asparagus during a harvesting process based on discrete element method. Biosyst. Eng. 196:127-144.

Leblicq, T., Smeets, B., Ramon, H., Saeys, W., 2016a. A discrete element approach for modelling the compression of crop stems. Comput. Electron. Agric. 123:80-88.

Leblicq, T., Smeets, B., Vanmaercke, S., Ramon, H., Saeys, W., 2016b. A discrete element approach for modelling bendable crop stems. Comput. Electron. Agric. 124:141-149.

Mu, L.T., Liu, H.Z., Cui, Y.J. 2018. Mechanized technologies for scaffolding cultivation in the kiwifruit industry: a review. Inf. Process. Agric. 5:401-410.

Ma, Y.H., Song, C.D., Xuan, C.Z. 2020. Parameters calibration of discrete element model for alfalfa straw compression simulation. Trans. Chin. Soc. Agric. Eng. 36:22-30.

Suo, R., Gao, F.F., Zhou Z.X., Fu, L.S., Song, Z.Z., Dhupia, J., Cui, Y.J. 2020. Improved multi-classes kiwifruit detection in orchard to avoid collisions during robotic picking. Comput. Electron. Agric. 182:106052.

Schramm, M., Tekeste, M.Z., 2022. Wheat straw direct shear simulation using discrete element method of fibrous bonded model. Biosyst. Eng. 213:1-12.

Sadrmanesh V., Chen, Y. 2018 Simulation of tensile behavior of plant fibers using the discrete element method (DEM). Compos. Part A-Appl. S. 114:196-203.

Sadek, M.A., Chen, Y., Lagu,C. 2011. Characterization of the shear properties of hemp fiber and core using the discrete element method. Trans. ASABE 54:2279-2285.

Ucgul, M., Saunders, C., Fielke, J.M., 2017. Discrete element modelling of top soil burial using a full scale mouldboard plough under field conditions. Biosyst. Eng. 160:140-153.

Yuan, J. 2020. Research progress analysis of robotics selective harvesting technologies. Trans. Chin. Soc. Agric. Machin. 51:1-17.

Zeng, Z.W., Ma, X., Cao, X.L., Li, R.H., Wang, X.C. 2021. Critical review of applications of discrete element method in agricultural engineering. Trans. Chin. Soc. Agric. Machin. 52:1-20.

Zhang, S.L., Zhao, H.B., Wang X.Z., Dong J.X., Zhao, P.F., Yang F.F., et al. 2023. Discrete element modeling and shear properties of the maize stubble-soil complex. Comput. Electron. Agric. 204:107519.

Zhang, T., Zhao, M., Liu, F., Tian, H., Wulan, T., Yue, Y., Li, D., 2020. A discrete element method model of corn stalk and its mechanical characteristic parameters. Bioresources 15:9337-9350.

Zhang, B., Xie, Y., Zhou, J., Wang, K., Zhang, Z., 2020. State-of-the-art robotic grippers, grasping and control strategies, as well as their applications in agricultural robots: A review. Comput. Electron. Agric. 177:105694.

Zhao, W., Chen, M., Xie, J., Cao, S., Wu, A., Wang, Z., 2023. Discrete element modeling and physical experiment research on the biomechanical properties of cotton stalk. Comput. Electron. Agric. 204:107502.

Wang, Y., Zhang, Y.T., Yang, Y., Zhao, H.M., Yang, C.H., He, Y., et al. 2020. Discrete element modelling of citrus fruit stalks and its verification. Biosyst. Eng. 200:400-4.

Williams, H., Jones, M.H., Nejati, M., Seabright, M.J., Bell, J., Penhall, N.D., et al. 2019. Robotic kiwifruit harvesting using machine vision, convolutional neural networks, and robotic arms. Biosyst. Eng. 181:140-156.

Williams, H., Nejati, M., Hussein, S., Penhall, N., Lim, J.Y., Jones, M.H., et al. 2020. Autonomous pollination of individual kiwifruit flowers: Toward a robotic kiwifruit pollinator. J. Field Robot 37:246-262.

Wang, J., Xu, C., Xu, W., Fu, Z., Wang, Q., Tang, H., 2022. Discrete element method simulation of rice grain motion during discharge with an auger operated at various inclinations. Biosyst. Eng. 223:97-115.

Wang, X., Li, P., He, J., Wei, W., Huang, Y. 2021. Discrete element simulations and experiments of soil-winged subsoiler interaction. Int. J. Agric. Biol. Eng. 14:50-62.

Wu, K., Song, Y. 2022. Research progress analysis of crop stalk cutting theory and method. Trans. Chin. Soc. Agric. Machin. 53:1-20.